AD-A142 474 BIOLOGICAL EFFECTS OF MILLIMETER-WAVE IRRADIATION: 1/1
LIVING BACTERIAL ORGAN..(U) UTAH UNIV SALT LAKE CITY
DEPT OF ELECTRICAL ENGINEERING O P GANDHI ET AL.
UNCLASSIFIED APR 84 UTEC-83-84004 USAFSAM-TR-84-11 F/G 6/18 NL

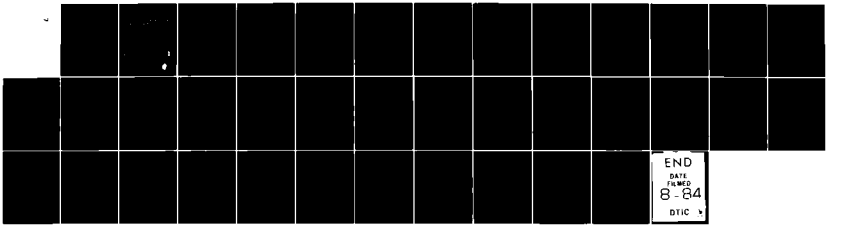

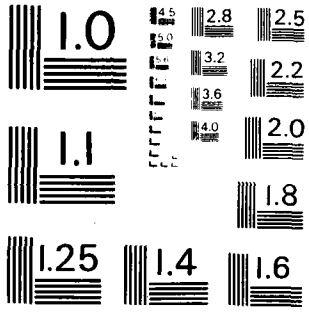

(12)

Report USAFSAM-TR-84-11

BIOLOGICAL EFFECTS OF MILLIMETER-WAVE IRRADIATION: LIVING BACTERIAL ORGANISMS

O. P. Gandhi, Sc.D.
D. W. Hill, Ph.D.
L. Furia, M.S.
M. F. Iskander, Ph.D.
D. Ghodgaonkar, M.S.
A. Riazi, Ph.D.
C. H. Wang, Ph.D.

Department of Electrical Engineering
University of Utah
Salt Lake City, Utah 84112

April 1984

Final Report for Period 15 July 1982 - 14 October 1983

Prepared for
USAF SCHOOL OF AEROSPACE MEDICINE
Aerospace Medical Division (AFSC)
Brooks Air Force Base, Texas 78235

NOTICES

This final report was submitted by the Department of Electrical Engineering, University of Utah, Salt Lake City, Utah 84112, under contract F33615-82-K-0631, job order 2312-V7-11, with the USAF School of Aerospace Medicine, Aerospace Medical Division, AFSC, Brooks Air Force Base, Texas. Dr. David N. Erwin (USAFSAM/RZP) was the Laboratory Project Scientist-in-Charge.

When Government drawings, specifications, or other data are used for any purpose other than in connection with a definitely Government-related procurement, the United States Government incurs no responsibility or any obligation whatsoever. The fact that the Government may have formulated or in any way supplied the said drawings, specifications, or other data, is not to be regarded by implication, or otherwise in any manner construed, as licensing the holder, or any other person or corporation; or as conveying any rights or permission to manufacture, use, or sell any patented invention that may in any way be related thereto.

The Office of Public Affairs has reviewed this report, and it is releasable to the National Technical Information Service, where it will be available to the general public, including foreign nationals.

This report has been reviewed and is approved for publication.

David N. Erwin

DAVID N. ERWIN, Ph.D.
Project Scientist

John C Mitchell

JOHN C. MITCHELL, B.S.
Supervisor

Royce Moser

ROYCE MOSER, Jr.
Colonel, USAF, MC
Commander

REPORT DOCUMENTATION PAGE

1a. REPORT SECURITY CLASSIFICATION: UNCLASSIFIED	1b. RESTRICTIVE MARKINGS
2a. SECURITY CLASSIFICATION AUTHORITY	3. DISTRIBUTION/AVAILABILITY OF REPORT: Approved for public release; distribution is unlimited.
2b. DECLASSIFICATION/DOWNGRADING SCHEDULE	
4. PERFORMING ORGANIZATION REPORT NUMBER(S): UTEC 83-84004	5. MONITORING ORGANIZATION REPORT NUMBER(S): USAFSAM-TR-84-11
6a. NAME OF PERFORMING ORGANIZATION: Dept. of Electrical Engineering, University of Utah; 6b. OFFICE SYMBOL (If applicable)	7a. NAME OF MONITORING ORGANIZATION: USAF School of Aerospace Medicine (RZP)
6c. ADDRESS (City, State and ZIP Code): Salt Lake City, Utah 84112	7b. ADDRESS (City, State and ZIP Code): Aerospace Medical Division (AFSC), Brooks Air Force Base, Texas 78235
8a. NAME OF FUNDING/SPONSORING ORGANIZATION; 8b. OFFICE SYMBOL (If applicable)	9. PROCUREMENT INSTRUMENT IDENTIFICATION NUMBER: F33615-82-K-0631
8c. ADDRESS (City, State and ZIP Code)	10. SOURCE OF FUNDING NOS.

PROGRAM ELEMENT NO.	PROJECT NO.	TASK NO.	WORK UNIT NO.
61102F	2312	V7	11

11. TITLE (Include Security Classification): BIOLOGICAL EFFECTS OF MILLIMETER-WAVE IRRADIATION: LIVING BACTERIAL ORGANISMS

12. PERSONAL AUTHOR(S): Gandhi, O.P.; Hill, D.W.; Furia, L.; Iskander, M.F.; Ghodgaonkar, D.; Riazi A.; Wang, C. H.

13a. TYPE OF REPORT	13b. TIME COVERED	14. DATE OF REPORT (Yr., Mo., Day)	15. PAGE COUNT
Final Report	FROM 15 Jul 82 TO 14 Oct 83	1984 April	38

16. SUPPLEMENTARY NOTATION

17. COSATI CODES			18. SUBJECT TERMS (Continue on reverse if necessary and identify by block number)
FIELD	GROUP	SUB. GR.	
06	15		Millimeter waves; Saccharomyces cerevisiae; Mutagenic effects; Bacillus megaterium; Infinite sample method; In vivo measurements

19. ABSTRACT (Continue on reverse if necessary and identify by block number)

The report describes experiments on the effects of millimeter-wave irradiation on the mutation rates of Salmonella typhimurium strains TA 1535 and TA 1538. No frequency-sensitive irradiation effects have been observed in spite of closely spaced frequencies used in the 42-48 and 65-75 GHz bands. Some preliminary experiments performed with yeast Saccharomyces cerevisiae have given rates of growth that are dependent on the irradiation frequency.

However, on account of the high degree of variability, accurate frequency resettability is a must before firm conclusions can be drawn. A new method for measuring complex permittivities of biological media in vitro and in vivo has been proposed and tested for feasibility. Raman laser spectroscopy is proposed as a means of searching for frequency-specific biological effects of millimeter-wave irradiation. The Raman system setup for these studies is used for pilot studies with vesicular stomatitis, Sindbis, and LaCrosse viruses and with Bacillus megaterium.

20. DISTRIBUTION/AVAILABILITY OF ABSTRACT	21. ABSTRACT SECURITY CLASSIFICATION	
UNCLASSIFIED/UNLIMITED ☒ SAME AS RPT. ☐ DTIC USERS ☐	UNCLASSIFIED	
22a. NAME OF RESPONSIBLE INDIVIDUAL: David N. Erwin, Ph.D.	22b. TELEPHONE NUMBER (Include Area Code): (512) 536-3582	22c. OFFICE SYMBOL: USAFSAM/RZP

DD FORM 1473, 83 APR — EDITION OF 1 JAN 73 IS OBSOLETE.

18. SUBJECT TERMS (continued)

Laser Raman spectroscopy of biological media; Vesicular Stomatitis, Sindbis, and LaCrosse viruses; Brillouin and Raman spectroscopy of biological media; Salmonella typhimurium; Complex permittivities.

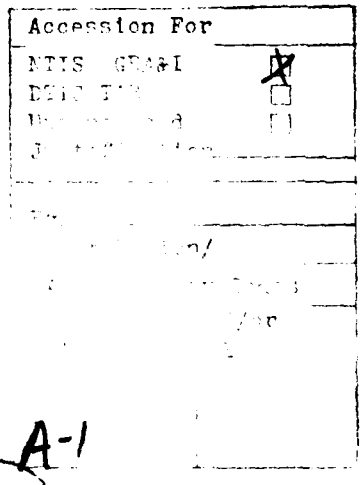

BIOLOGICAL EFFECTS OF MILLIMETER-WAVE IRRADIATION: LIVING BACTERIAL ORGANISMS

INTRODUCTION

With the recent and projected advances in millimeter-wave technology, including the availability of high-power transmitters in this band, it has become necessary to understand the interaction of fields at these frequencies with living organisms. Several research reports [1-4] indicate sharp millimeter-wave frequency-dependent lethal and mutagenic effects on microorganisms, and effects on growth of cells. In the absence of basic knowledge of the dielectric properties of biological media, it is difficult to judge the validity of these claims or to guess about the frequency regions of greatest interest. To search for frequency-specific effects, evaluation of the action spectra of millimeter-wave irradiation is inefficient, relying as it does on fairly time-consuming biological and biochemical assays. One such study undertaken by us for protein synthesis by baby hamster kidney (BHK) mammalian cells [5-7] with and without continuous-wave (CW) irradiation, for 202 frequencies at 0.1-GHz intervals in the 38- to 48-GHz and 65- to 75-GHz bands, failed to reveal any microwave-induced effects as compared to control samples. Further studies, conducted by our group as a part of the present project, have also failed [8] to show athermal mutagenic effects of millimeter-wave radiation for the following systems:

1. Induction in Escherichia coli of strains of wild-type lambda phage sensitive to mutation to mitomycin C and ultraviolet light but insensitive to induction at temperatures as high as 39°C.
2. Induction in Escherichia coli of temperature-sensitive (ts) mutants of lambda phage characterized and tested with regard to thermal sensitivity of induction in the 32-42°C range and to response to ultraviolet light.
3. Salmonella typhimurium strain TA 1538 (His^- mutant due to frame shift mutation).

4. Salmonella typhimurium strain TA 1535 (His^- mutant due to base pair mutation).

All of the above strains have been irradiated with the use of the broadband temperature-controlled irradiation system [9] designed and built as a part of this project. This system allows simultaneous irradiation and sham irradiation of cell cultures under flowing conditions while keeping the temperature difference between radiated and control samples to within ±0.02°C.

Some research reported in this area [2, 3] has emphasized the use of highly stabilized millimeter-wave sources (stabilized to within ±0.1 MHz) as a necessary requirement for the observation of resonant-type biological effects. During the current year of the project we have used a highly stable klystron source (stabilized to within ±0.15 MHz) to irradiate exponentially growing cultures of Saccharomyces cerevisiae at frequencies around 41.84 GHz. Preliminary results described in the next section seem to indicate a possible presence of perturbations on the growth rate due to millimeter-wave irradiation. These experiments have also pointed to a need for accurate frequency resettability which has not been possible in our present system. An accurate stabilizer system and a frequency counter similar to the one used by previous researchers are therefore needed for the experiments before definite conclusions can be drawn.

Using conventional approaches, accurate measurements of the complex permittivities of the biological media have been difficult at millimeter wavelengths requiring precisely fabricated sample holders [10, 11] covering fairly narrow bandwidths. Also, because of very high attenuation constants on the order of 150-300 dB/cm, the thickness of the conventional sample holders has had to be a fraction of a millimeter, with concomitant problems of air bubbles and nonuniform filling densities for biological tissues. We are developing new and novel approaches which will alleviate these problems, making it possible to obtain the absolute permittivities of the biological tissues over the 26.5-to 90-GHz band for which the solid-state computer-controlled precision measurement facilities [12] are currently available in our laboratory. Knowledge of complex permittivities of biological preparations and tissues is needed for dosimetry and is valuable in anticipating any frequency-specific effects.

An important area of research in the area of radiofrequency radiation (RFR) bioeffects is to determine the mechanisms of interaction between electromagnetic fields and biological entities. A promising line of investigation suggested toward this objective is the laser Brillouin and Raman spectral studies. Laser Brillouin spectroscopy has the advantage of being able to emit (launch) or absorb acoustic phonons in a medium at frequencies on the order of 0.0-1.0 cm^{-1} (3 to 30 GHz). For higher frequency optical phonons ($\geq$ 5-10 cm^{-1}), Raman spectroscopy is more appropriate. The dimensions of biological macromolecules and cells are of the order of several tens to thousands of Ångstroms and comparable to the wavelength of acoustic waves at microwave/millimeter frequencies in these structures. It is entirely conceivable, therefore, that Brillouin and Raman spectral studies will provide a new and useful means of studying these media, particularly regarding the mechanisms of interaction at microwave frequencies. Fröhlich [13] has alluded to the possibility of specific frequencies of a biological system related to the excitability of acoustic phonons in cells. It is proposed to use the Raman spectroscopy as a physical tool for real-time evaluation of frequency-specific effects of millimeter-wave irradiation. The bioassays used by us [5-7] and others are fairly time consuming to search for frequency-specific effects and have a disadvantage that bioeffects during irradiation, if any, are not detected by lack of concurrency of the techniques.

MUTAGENIC EFFECTS OF MILLIMETER-WAVE IRRADIATION

Effects on Salmonella Typhimurium

The irradiation system [9] developed on this project was used to continue probing the possible mutagenic effects of millimeter-wave irradiation upon living bacterial organisms. After having tested for induction in Escherichia coli of wild-type and temperature-sensitive mutants of lambda phage in the past year, we used two mutant strains of Salmonella typhimurium to further investigate the possible mutagenicity of millimeter waves. These two strains, TA 1535 and TA 1538, were chosen because both possess a His^- mutation; the strain TA 1535 due to a base pair mutation and the strain TA 1538 due to frame shift mutation. These are also the typical mutants used in mutagenicity tests

of biochemicals and ionizing radiation, as described in the original Ames papers [14, 15]. The availability of two different strains, both lacking the capability of synthesizing histidine but due to two distinctly different mutagenic mechanisms (base pair and frame shift), has been judged of high interest in order to cover various, possible, back-mutations mechanisms induced by the millimeter-wave irradiation. Both strains were assayed for response to ultraviolet light and to crystal violet, for the rate of spontaneous back mutations, and for growth in presence of histidine. The mutagenic test used has been the standard Ames test [15]. The experimental conditions are as follows:

An aliquot of stock culture was inoculated in 50 ml of L-broth (tryptone 10 g/l, NaCl 5 g/l, yeast extract 5 g/l) and allowed to grow for 18-22 hr on a stirrer at room temperature. Before starting the irradiation, the millimeter-wave system was warmed for at least 45 min and both incident power and irradiation frequency checked. The closed-loop circuits for the irradiated and sham-irradiated cultures were loaded and, after the thermal equilibrium was reached between the two cultures, the actual irradiation was started.

Using the temperature-compensating system, the temperature difference between the two circuits was maintained to within ±0.02°C. The parameters of the irradiation have been the following:

a. 30 min of irradiation,
b. square-wave modulation with a modulation frequency of 1000 Hz,
c. the frequency ranges were 40.5 to 46.5 GHz and 65.0 to 75.0 GHz for the TA 1538 strain and 42.0 to 48.0 GHz and 65.0 to 74.0 GHz for the TA 1535 strain,
d. the frequency step was 0.5 GHz,
e. the incident power in the waveguide was in the ranges 3-10 mW and 10-14 mW for the U-band (40-48 GHz) and E-band (65-75 GHz) respectively,
f. the cultures were kept at 37.0°C ± 0.04°C during the irradiation, and
g. for each frequency at least three experiments were conducted.

After the irradiation, the suspensions from each circuit were collected and a 0.1-ml aliquot of each was placed in a tube containing 2 ml of "Top" agar (agar 6 g/l, NaCl 6 g/l) containing the proper amount of histidine. We used the amount of histidine described in the original Ames protocol [15] for

the strain TA 1535 (i.e., 10 ml of histidine, 0.5 mM for each 100 ml of Top Agar), while we used a smaller amount, 2.5 ml of histidine 0.5 mM in 100 ml of Top Agar, for the strain TA 1538. This was necessary because with the original amount we obtained too many colonies for the TA 1538 strain.

The original culture so diluted was then thoroughly stirred in a tube and poured on Vogel Bonner Essential (VBE) agar plates (VBE 50 X solution 20 ml/l, agar 15 g/l, glucose 20 g/l). After a 48-hr incubation at 37°C, the resulting back-mutation colonies were counted. The differences in the number of revertant colonies of the irradiated and the sham-irradiated cultures were plotted versus the irradiation frequency.

The data in Figures 1 through 4 show the average of all of the runs for the indicated frequencies and the standard deviation calculated with the expression for small numbers of samples

$$\sigma = \left[\sum_{i=1}^{N} \frac{\left(x_i - \bar{x} \right)^2}{N - 1} \right]^{1/2} \qquad (1)$$

These data show that no significant difference could be detected under the above-described conditions between cultures of Salmonella typhimurium, strain TA 1538 and TA 1535, irradiated and sham-irradiated with millimeter waves while kept under isothermal conditions. The smaller standard deviation present in the data for the TA 1538 strain was ascribed to a smaller variability of spontaneous back-mutation rate for the strain TA 1538 as against that for the TA 1535 strain.

In addition to the above-reported experiments whose irradiation duration was always 30 min, additional experiments were conducted for longer periods (1 and 2 hr) on the TA 1538 strain at selected frequencies. These frequencies (66.0, 69.5, 70.5 GHz) were chosen because, for the shorter-term (30 min) exposures, a somewhat lower number of back-mutation revertants were observed for the irradiated samples. The decision to make the additional runs was motivated by a desire to cover more than one generation time, which for the TA 1538 is about 40 min. But for the exposure time all of the other experimental parameters were the same as in the earlier experiments. Even for these

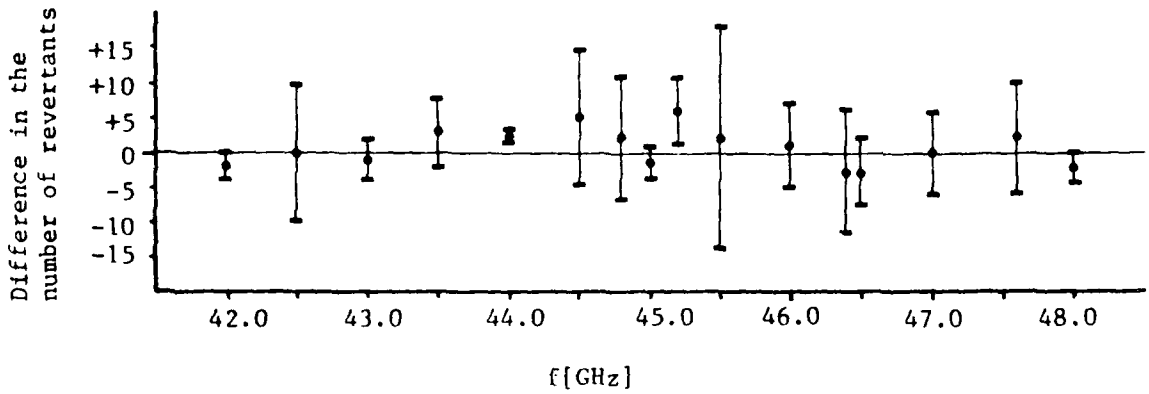

Figure 1. The difference between the number of revertant colonies of the irradiated and sham-irradiated cultures for Salmonella typhimurium TA 1535 in the U-band.

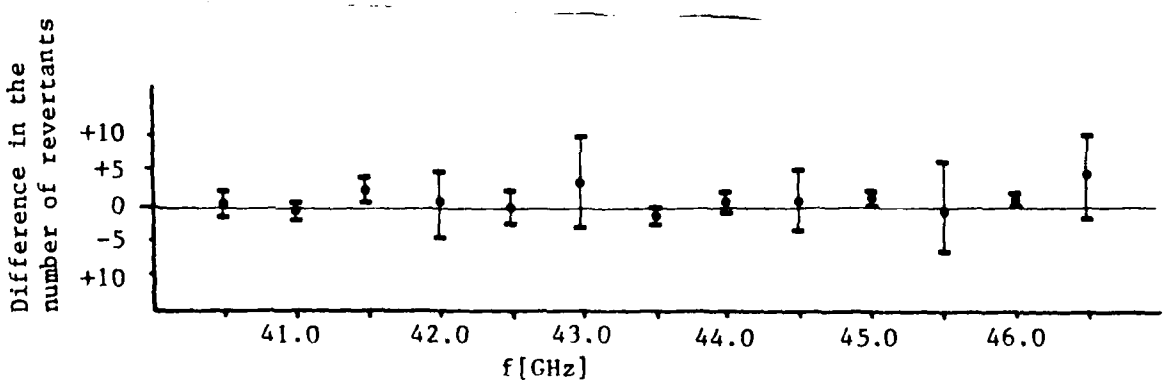

Figure 2. The difference between the number of revertant colonies of the irradiated and sham-irradiated cultures for Salmonella typhimurium TA 1538 in the U-band.

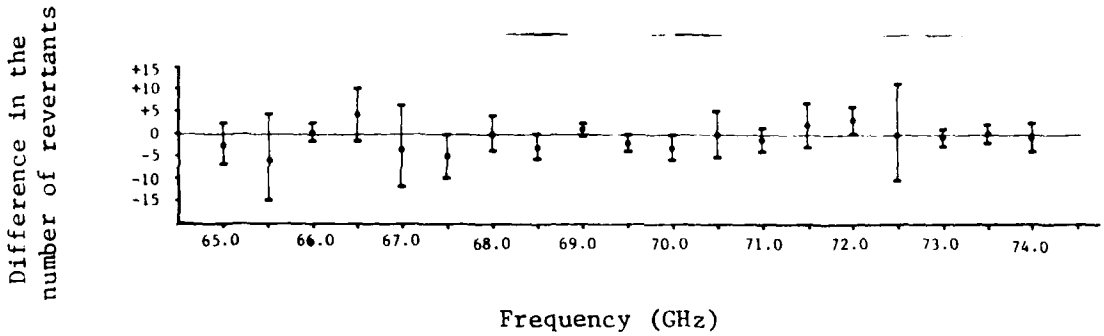

Figure 3. The difference between the number of revertant colonies of the irradiated and sham-irradiated cultures for Salmonella typhimurium TA 1535 in the E-band.

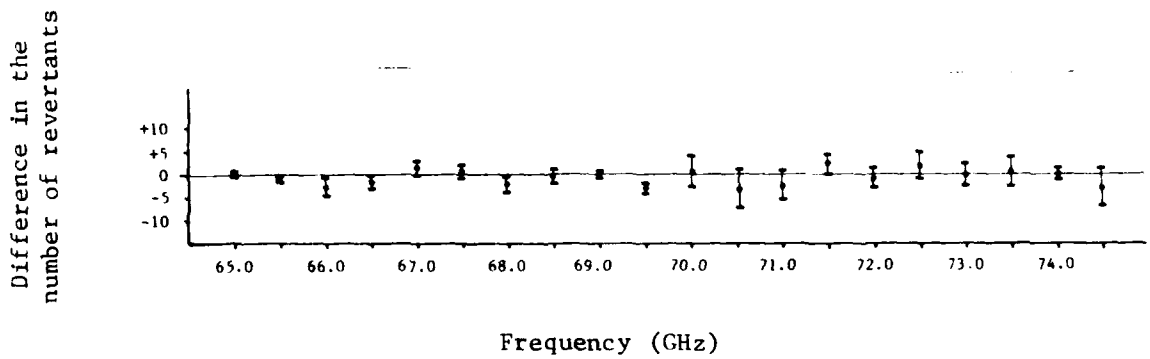

Figure 4. The difference between the number of revertant colonies of the irradiated and sham-irradiated cultures for Salmonella typhimurium TA 1538 in the E-band.

experiments, no significant differences in the number of back-mutation revertants were observed. The data relative to this experiment are shown in Table 1.

TABLE 1. NUMBER OF REVERTANTS OF SALMONELLA TYPHIMURIUM TA 1538 AS A FUNCTION OF THE IRRADIATION FREQUENCY AND EXPOSURE TIME IN THE E-BAND

F [GHz]	Duration of irradiation		
	30 min	60 min	120 min
66.0	-3.0 ± 2.6	-0.33 ± 0.57	+2.0 ± 1.0
69.5	-3.0 ± 0.6	+0.33 ± 2.1	-3.0 ± 0.0
70.5	-3.6 ± 4.2	0.0 ± 1.0	-1.0 ± 0.0

Search for Resonant Effects on the Growth Rate of Yeast Cultures Exposed to Millimeter-Wave Irradiation

Grundler et al. [2, 16, 17] have reported resonant effects on the growth rates of Saccharomyces cerevisiae due to millimeter-wave irradiation in the range 41.600-41.850 GHz. These resonances have been claimed as experimental evidence of the Fröhlich hypothesis regarding the presence of cooperative phenomena in living organisms [13]. The interpretations reported in references 2, 16, and 17 have, however, not been universally accepted due possibly to the following factors:

1. The graphs represented in an earlier paper [2] showed a large scattering of the experimental data that had been connected with a resonant-like continuous curve that often took into account only the larger of the deviations. Their latest paper [17] represents, however, the results of nearly 300 experiments performed with two different exposure systems over a period of several years.
2. The reported periodic resonances with a claimed bandwidth of 10 MHz are often represented by peaks whose values are not considered biologically significant (often less than ±8% variation with respect to the control growth rates).
3. The irradiation system (a Teflon® fork-shaped antenna immersed in the cell suspension) does not have a well-characterized irradiation pattern leading, therefore, to the difficulty of defining the dose distribution pattern.

4. The photometric system used to monitor continuously the growth rate takes into account the possible dead cells, and thus cannot be considered a viability test.
5. The control cell cultures were not sham-exposed simultaneously in the earlier set of experiments leading, therefore, to a potential for natural variation in the growth rates.

We have decided to use the following solutions to resolve at least in part some of the criticisms of Grundler's work:

1. The experimental data for each experiment have been fitted to an exponential curve using the least square methods. The exponential growth rates thus obtained are shown.
2. After determining the experimental variability of our protocol, we decided to consider only those experiments significant for which the percentage difference is larger than ±10%.
3. We employed the dosimetrically quantifiable irradiation system [9] built for this project and already used for the mutagenic experiments reported in the preceding section of this report. Among other features, this system has an irradiation pattern that is defined theoretically and checked experimentally.
4. In order to measure the growth rate of yeast, we used a measure of viability, taking a sample of the cultures just before the irradiation and hourly thereafter. The data were fitted to an exponential curve for which the growth rate was obtained by the least square method.
5. The irradiation system we used allows simultaneous irradiation and sham-irradiation of two cultures that are placed in identical environments.

Besides minimizing the previously stated criticisms, we complied with the three main features emphasized by Grundler et al. [2, 16, 17] for resonant effects. These requirements are:

1. Frequency stability both on short- and long-term (4 hr) bases.
2. Resettability of the operating frequency and high accuracy of its measurement.

3. Imposing to the control cultures the same temperature variations as those for the irradiated cell- while at the same time making all the possible efforts to keep both temperatures within a close range (within ±0.02°C) around the chosen experimental temperature.

We used the following procedures to have control of these characteristics:

1. We used a normal (not frequency stabilized) klystron (OKI 40V12) and continuously monitored its output frequency with a spectrum analyzer. The short-term frequency stability for the OKI 40V12 klystron is ≈ ±150 kHz, including also the instability of the local oscillator of the spectrum analyzer. We used a manual feedback on the cavity dimensions and/or on the reflector voltage to compensate for the frequency shifts during irradiation. In order to keep track of the frequency shift, we employed a custom-made frequency-shift recorder fed with the outputs of the spectrum analyzer (sawtooth and video). This frequency-shift recorder well exceeded the minimal requirements of sensitivity and stability needed for these experiments. It was, in fact, capable of sensing a frequency shift of 50 kHz for frequencies on the order of 40 GHz (≈ 1 ppm). The frequency stability (±150 kHz) is better than the frequency stability reported in references 2 and 16, that was ±1 MHz. The stability of the klystron is achieved both by keeping the environmental temperature in the 20-26°C range and employing a very careful tuning technique. This includes, for example, operating the klystron well below its rated power, careful setting of the grid voltage, and a warmup time of not less than 1.5 hr. A greatly increased frequency stability on the order of ±100 Hz may be achieved by a state-of-the-art frequency-stabilized millimeter-wave generator.
2. Frequency resettability for the present experiments was obtained by using a 16-in wood case lined with Styrofoam to hold the cavity-type frequency meter. A resistive heater and a temperature probe connected with a proportional temperature controller (YSI 72) were within this case, in close contact with the frequency meter. Even though the YSI 72 has a sensitivity of 0.01°C, the time constant of

the whole system imposed a temperature stability of +0.07°C and -0.03°C. The chosen operational temperature was 31.0°C, the same as in references 2 and 16. In order to check the mechanical resettability of the frequency meter, its resonant frequency had to be undertaken through wide excursions several times (≈ 10) while feeding it with a signal monitored on the spectrum analyzer. Using this procedure, the resulting mechanical resettability was determined to be ±3.0 MHz.

3. We employed the irradiation system described in reference 9 and previously used for the mutagenic effects study of this project. This system allowed us to keep the control cultures within ±0.02°C from the temperature of the irradiated cultures.

The block diagram of the system is shown in Figure 5. We performed a four-way analysis of variance on the experimental data in order to ascertain the statistical significance of the results. The actual experimental conditions are hereby described.

An aliquot of stock culture of Saccharomyces cerevisiae was inoculated in 50 ml of Sabouraud glucose broth (glucose 20g/l, Neopeptone 10 g/l). The cells were grown for 18-32 hr on a stirrer at 32°C. Before loading the circuits, the cultures were usually diluted 1:10 or 1:100 in order to have an approximate initial concentration of 10^5-10^6 cells/ml. The two circuits were then loaded with 5 ml of culture each by filling the respective storage tubes. The necessity for using these storage tubes stems from the need to have enough volume for the hourly sampling of 0.2 ml and still have enough suspension to fill the circuits. The tubes are provided with filtered air to stir and aerate the cultures.

After at least 1.5 hr, the irradiation was begun; this time lag was necessary both for the warmup of the millimeter-wave system and for the cells to enter the log phase. The peristaltic pump was checked and adjusted for each experiment to a flow rate of 5 ml/min. This gave an exposure time of 3.1 sec for a sample of the suspension to pass through the sample holder, while the repetition rate is 1 min. The irradiation time was 4 hr with continuous wave at a power in the waveguide of 20 mW ± 0.1 mW. At the beginning of the irradiation and every hour thereafter, an aliquot of 0.2 ml was taken from

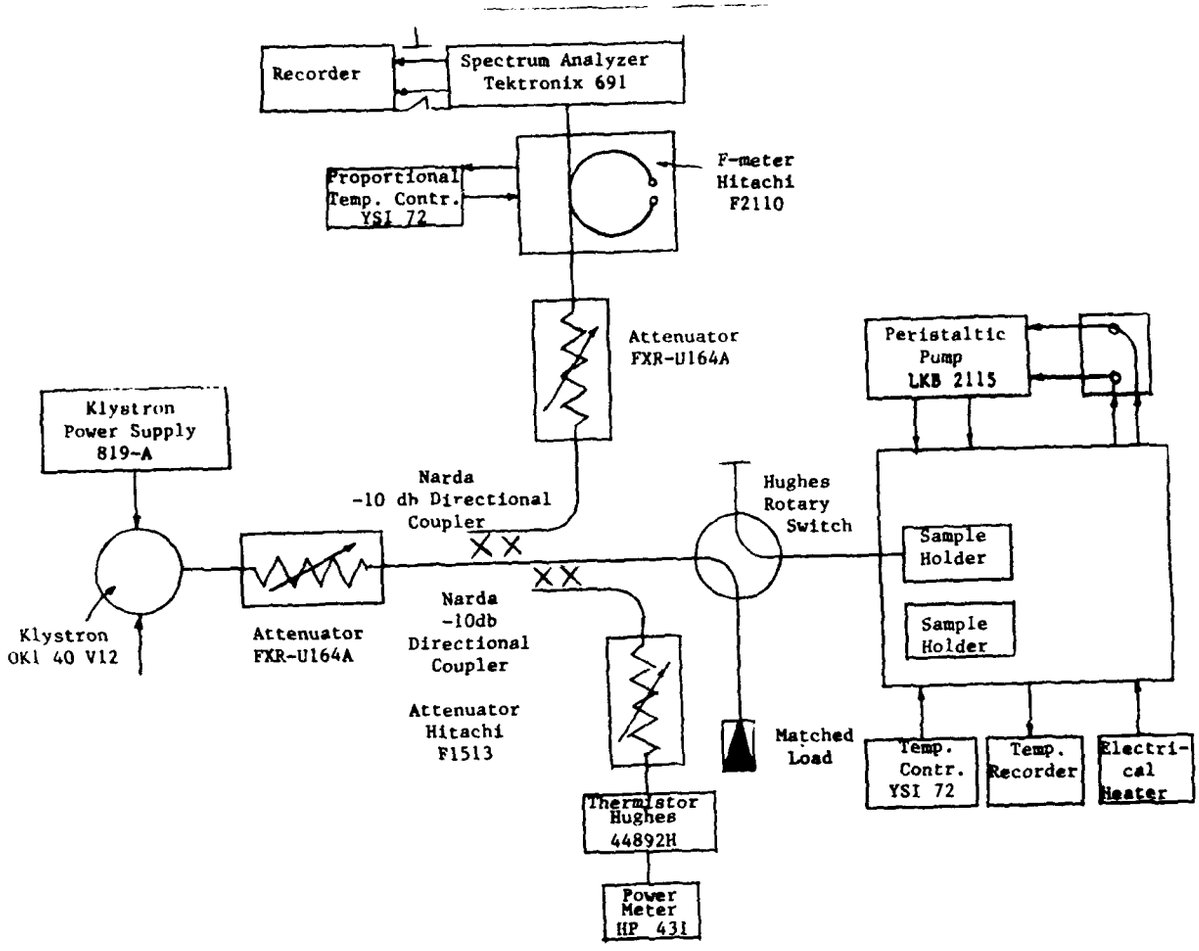

Figure 5. Block diagram of the irradiation system used for the Saccharomyces cerevisiae experiments.

the storage tube, diluted 10:4 in Sabouraud glucose broth, and plated on 4 or 6 Sabouraud glucose agar plates (Bacto Agar 15 g/l, glucose 40 g/l, Neopeptone 10 g/l) for each culture. The plates were then incubated for 48 hr at 32°C. The results were averaged for each set of 4 or 6 plates and the resulting data fitted for an exponential curve.

Various experiments have been performed without millimeter-wave irradiation in order to check the overall effects of: (a) variation of two-cell suspensions placed in similar environments (i.e., the two channels of the irradiation chamber), and (b) the variability introduced by the plate-counting technique. In none of these experiments was the percent difference between the slopes of the two cultures greater than 8%. We can thus say that the chosen counting technique is accurate to within ±10%.

We began the experiments having planned to scan various closely spaced frequencies; however, the results of the first experiments (done with the air bubbling system) were fairly scattered around the baseline for a given frequency. Analyzing all the data for each experiment, the only known parameter that was changing among the various runs was the initial concentration.

We have thus decided to plot the percentage difference in growth rate vs. initial concentration, for a given frequency. The results are shown in Figures 6-8. Figures 6 and 7 refer to a frequency of 41.840 GHz, and the results are separated according to the number of plates used for each sampling (4 or 6). A split plot analysis of variance performed on the available data showed a statistically significant difference between irradiated and between radiation and replication, meaning that for various replication the presence of radiation induced a significant effect on the growth rate. A summary of the results of the statistical analysis is presented in Table 2.

PRECISION MEASUREMENTS OF THE COMPLEX PERMITTIVITIES OF BIOLOGICAL TISSUES

During the last year, we basically pursued two tasks:

1. Development of a semiautomated, modified "infinite" sample method to measure the complex permittivities of biological tissues and preparations. These efforts included further development of our X-band preliminary system and using this experience in the development of and actually making measurements on the millimeter-wave setup.

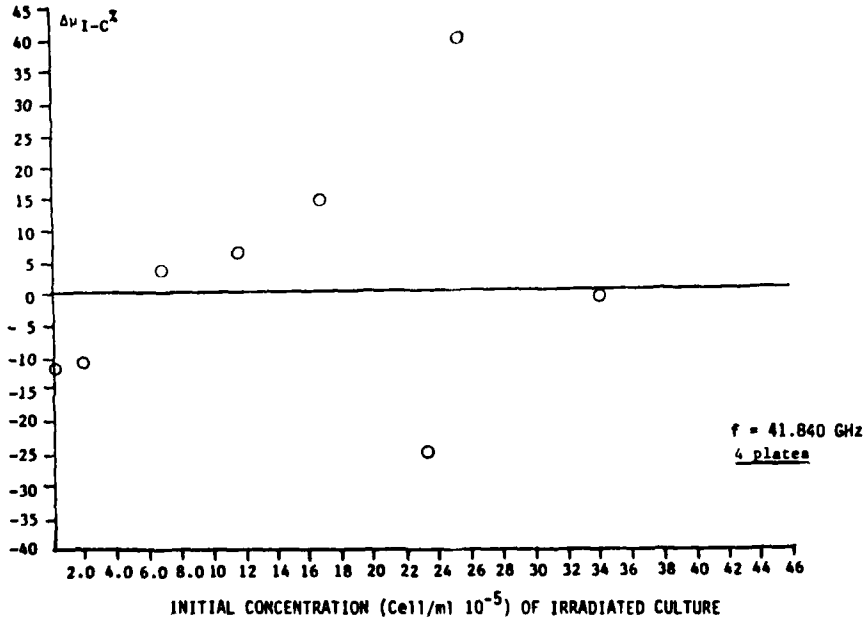

Figure 6. Percentage difference in growth rate vs. initial concentration for Saccharomyces cerevisiae exposed for 4 hr to millimeter-wave irradiation.

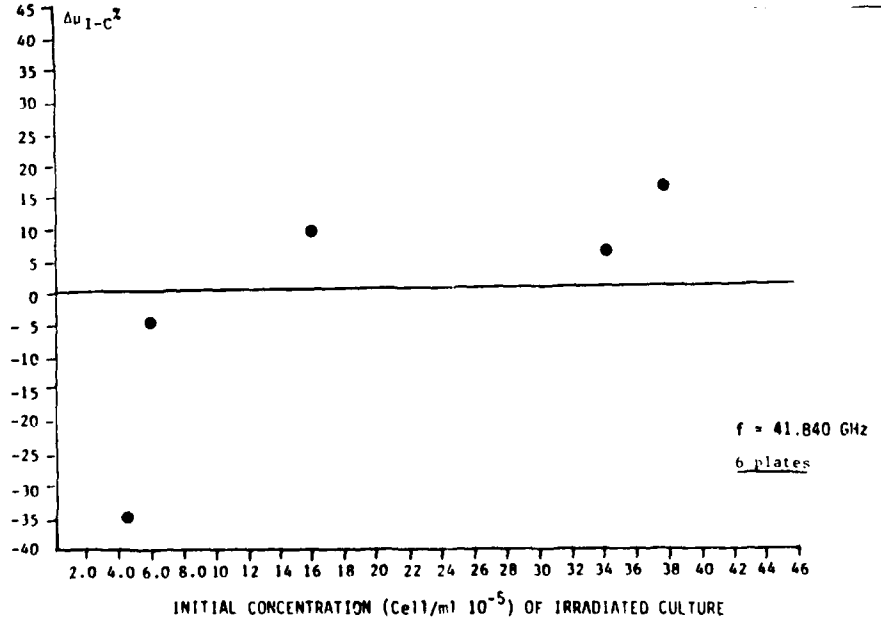

Figure 7. Percentage difference in growth rate vs. initial concentration for Saccharomyces cerevisiae exposed for 4 hr to millimeter-wave irradiation.

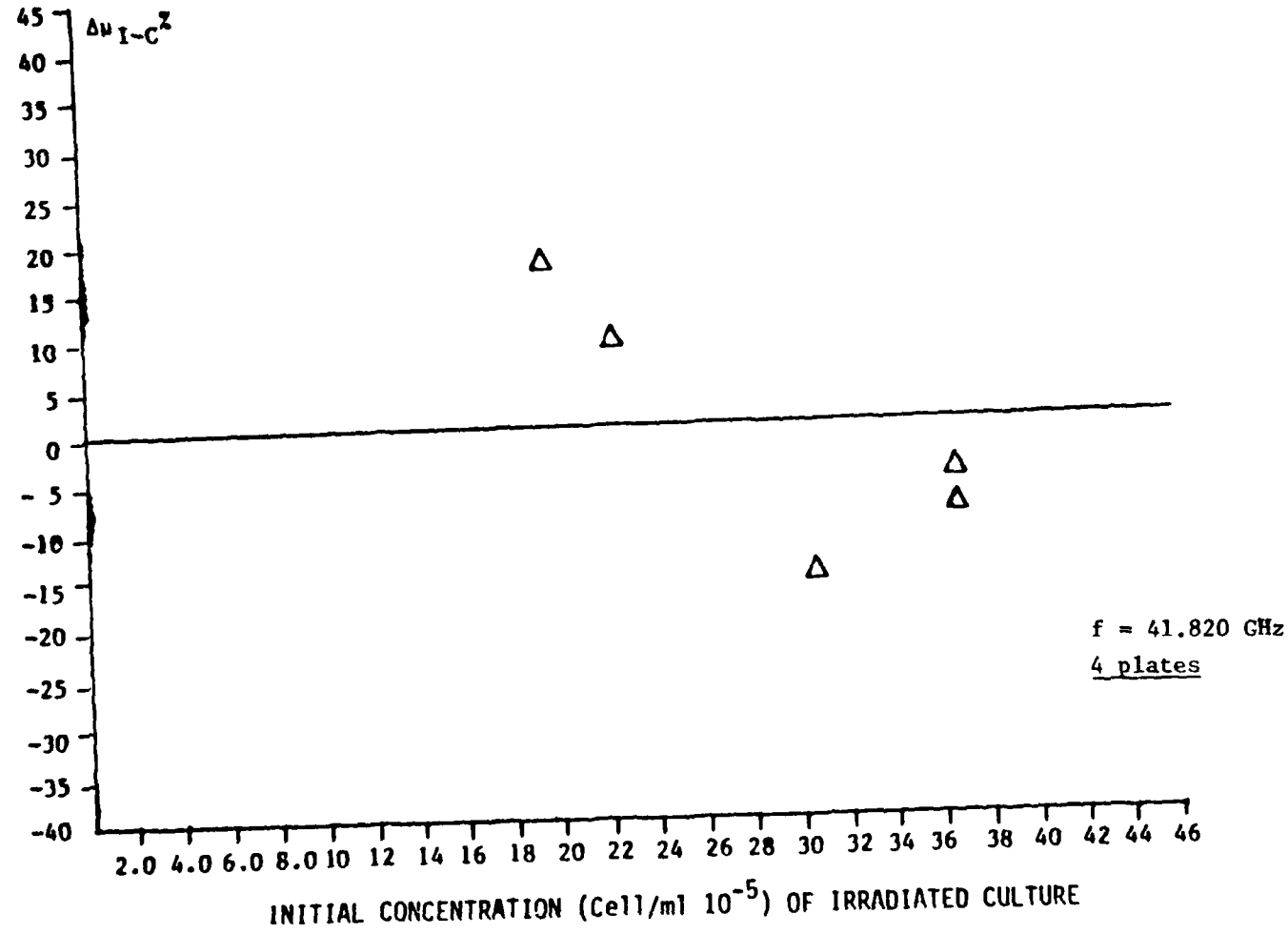

Figure 8. Percentage difference in growth rate vs. initial concentration for Saccharomyces cerevisiae exposed for 4 hr to millimeter-wave irradiation.

TABLE 2. SOME STATISTICAL RESULTS OBTAINED WITH A SPLIT PLOT ANALYSIS OF VARIANCE

f [GHz]	No. of Plates	No. of Experiments	Effect of Radiation	Effect of Replication	Effect of Interaction Of Rad*Rep
41.820	4	5	F = 8.68 df = 1/120 P < 0.01	F = 40.4 df = 4/120 P < 0.01	F = 17.5 df = 4/120 P < 0.01
41.840	4	7	F = 7.70 df = 1/168 P < 0.01	F = 20.7 df = 6/168 P < 0.01	F = 7.6 df = 6/168 P < 0.01
41.820	6	6	F = 0.002 df = 1/240 P > 0.05	F = 13.2 df = 5/240 P < 0.01	F = 23.4 df = 5/240 P < 0.01

2. Development of an in-vivo method for making these dielectric measurements in the millimeter-wave range. This development included theoretical efforts to relate the measured input admittance of the open-ended waveguide sample holder to the complex permittivity of the test sample.

We also performed experimental measurements to validate the adopted numerical method of solution. The following is a summary of the progress made in fulfilling these tasks.

Development of the Semiautomated Modified "Infinite" Sample Method

An analysis was performed to delineate the role of the dielectric constant of the intermediate layer on the inaccuracy in the calculated ε^* as a result of the errors in the measured values of the reflection coefficient $|\rho|$ and its phase $\angle\phi$. The results are shown in Table 3. It may be seen that the errors in the calculated values of ε^* are significantly lower for ε_I = 6.0 or 9.0 than for Teflon (ε_I = 2.1). A better match (lower $|\rho|$) between the biological tissues and the empty waveguide results, therefore, in an improved accuracy of the calculated complex permittivities. These higher dielectric constant materials were, therefore, ordered and used in our measurements.

TABLE 3. PERCENT ERROR IN COMPLEX PERMITTIVITY (ε^*) OF WATER FOR VARIOUS DIELECTRIC CONSTANTS (ε_I) AND LENGTHS (L) OF THE INTERMEDIATE LAYER

ε_I	Frequency GHz	$\frac{L}{\lambda_{g\varepsilon_I}}$	Reflection Coefficient $\lvert\rho\rvert$	Percent error in ε^* for ±1% error in $\lvert\rho\rvert$		Percent error in ε^* for ±1% error in $\lvert\phi\rvert$	
				Real Part	Imaginary Part	Real Part	Imaginary Part
2.1	10.05	0.25	0.588	3.16	5.25	3.59	-12.98
2.1	9.05	3.25	0.580	3.06	5.48	3.45	-13.81
6.0	9.9	0.25	0.070	0.25	0.38	0.28	-1.02
6.0	8.8	3.25	0.032	0.13	0.035	-0.025	-0.61
9.0	9.85	0.25	0.146	0.53	0.78	-0.58	2.17
9.0	8.75	3.25	0.197	0.60	1.59	-1.06	2.75

$\lambda_{g\varepsilon_I}$ *is the guide wavelength within the region of the waveguide occupied by the intermediate layer.*

Another point to note from Table 3 is that the length of the intermediate layer is of little consequence for the accuracy of the measurements. Thinner intermediate layers ($\ell \approx \lambda_{g\varepsilon I}/4$) were, therefore, used to reduce the losses associated with these "impedance transformers."

The intermediate layer is characterized for its dielectric constant using the short-circuited sample method [18]. This involves the use of a short placed immediately at the end of the intermediate layer sample of length ℓ. Measurements are made for the shift in locations of minima with and without the sample of ε_I.

If x_o is the measured shift in minima, then the dielectric constant is obtained from Equations 2-4.

$$\frac{\tan \beta_I \ell}{\beta_I \ell} = -\frac{\lambda_g}{2\pi\ell} \tan \frac{2\pi x_o}{\lambda_g} \qquad (2)$$

$$\lambda_{g\epsilon} = \frac{2\pi}{\beta_I} \tag{3}$$

$$\epsilon_I = \left(\frac{\lambda_o}{\lambda_c}\right)^2 + \left(\frac{\lambda_o}{\lambda_{g\epsilon}}\right)^2 \tag{4}$$

where λ_o and λ_c are the free-space wavelength and cutoff wavelength respectively. By this method, the dielectric constant of alumina for $\ell = 3\lambda_{g\epsilon I}/4$ is measured at several frequencies in the X-band. Frequency-averaged dielectric constant for X-band is measured to be 9.04. This measured value of dielectric constant is 3.83% below the desired value of 9.4. A reason for this discrepancy may be the improper accounting of the discontinuity at the air-dielectric interface. This reason and other possible sources or errors are presently being examined.

Errors in measurement of the reflection coefficient can be reduced by taking large numbers of voltage measurements along the slotted line at equal intervals and combining any three of these voltages to obtain the value of reflection coefficient. We decided to measure different sets of three voltages and to average the obtained values of the reflection coefficients. A computer program to implement the above-mentioned multiprobe method was developed on the Hewlett-Packard (HP) 9825 calculator. In order to implement the multiprobe method for measurement of complex reflectivities, however, it is required to move the detector along the slotted line at equal intervals by means of a stepping motor. Electronic circuitry required to control the movement of the stepping motor has been completed. The semiautomated measurement setup for the determination of dielectric properties is shown in Figure 9.

Some experience using the developed semiautomated multiprobe method was gained by making dielectric measurements in the frequency range from 9.8 to 11 GHz. The dielectric properties of deionized water and 0.9% saline thus obtained are compared in Table 4 with the theoretically obtained values. For the theoretical calculations, Debye equation was assumed and the following parameters were taken, $\epsilon_\infty = 4.9$, $\epsilon_s = 77.0$, and $\tau = 7.5 \times 10^{-12}$ sec.

It can be seen that the theoretical and experimental values for deionized water are within ±10% for real as well as for the imaginary parts of the

complex permittivity. Also, as expected, the imaginary part of complex permittivity for saline is higher than that for deionized water.

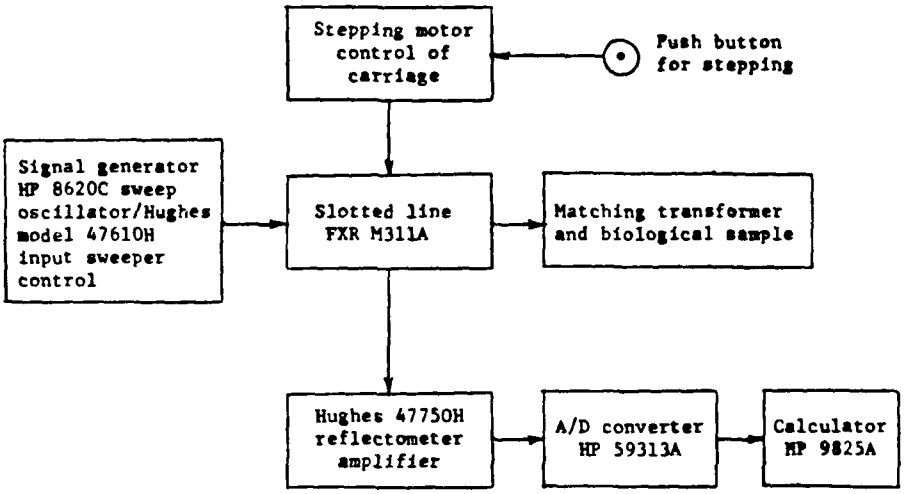

Figure 9. Block diagram of the measurement system for millimeter wavelengths.

In implementing the multiprobe method at millimeter wavelengths, we encountered some difficulties because of the fairly small size of the slotted line. Also, several other mechanical problems were experienced in fabricating the assembly that couples the movable probe to the stepping motor. Recently, however, we have designed and fabricated a new V-band slotted waveguide which is placed in the Universal probe carriage. Also a new detector probe was fabricated. With the placement of a new stepping motor, it was then possible to move the slotted line with step sizes from 0.005 ± 0.001 in to 0.04 ± 0.001 in. The number of steps along the slotted section of the waveguide was increased to 40-300 depending on the step size. It appears that the problem of uneven penetration of the probe has also been significantly reduced because the standard deviation of the reflection coefficient (magnitude $|\rho|$ and phase $\angle\phi$), as calculated from measurements of the standing wave pattern along the waveguide, was considerably lower. With the new slotted line-stepping motor

TABLE 4. COMPLEX PERMITTIVITIES FOR DEIONIZED WATER AND 0.9% SALINE

Frequency GHz	ε* theoretical from Debye equation		ε* for deionized water		ε* for 0.9% saline	
	Real part	Imaginary part	Real part	Imaginary part	Real part	Imaginary part
9.8	64.33	27.44	59.20	28.77	54.53	30.87
9.9	64.11	27.62	60.96	29.81	55.91	31.42
10.0	63.90	27.80	59.09	29.58	58.24	31.48
10.1	63.68	27.98	59.51	29.79	58.53	30.48
10.2	63.47	28.15	59.40	30.86	58.60	31.78
10.3	63.25	28.32	60.62	31.26	59.60	32.10
10.4	63.04	28.49	61.30	30.72	60.56	31.56
10.5	62.82	28.66	60.35	30.61	59.51	31.35
10.6	62.60	28.82	61.47	31.20	60.31	32.53
10.7	62.38	28.99	61.50	29.88	60.45	30.66
10.8	62.17	29.15	60.19	29.81	59.65	30.65
10.9	61.95	29.30	60.66	30.93	59.49	32.36
11.0	61.73	29.46	61.64	29.44	61.76	31.11

assembly, the experiments were performed for measurement of complex permittivity of water. The sample holder contained a 3.25 $\lambda_{g\epsilon I}$ matching transformer of $\epsilon_I = 6$ material.

On account of a somewhat lower detector sensitivity and consequently its lower output, the reflectometer amplifier and A/D converter in the measurement setup described in our last report were replaced by a regular voltage standing wave ratio (VSWR) meter and manual data entry. Also, a klystron (OKI-70V11) instead of solid-state Hughes oscillator was used to increase the incident power from 3 to 25 mW. After performing many measurements from 65 to 75 GHz, we draw the following conclusions:

a. The standard deviation in the measurement of $|\rho|$ and $\angle\phi$ using multiprobe method is significantly lower than our previous measurements.

b. The accuracy of measurements of $|\rho|$ and $\angle\phi$ has to be improved by either using a higher sensitivity detector diode, or modifying the detector mount, or increasing the incident power.

c. It is necessary to better characterize the matching transformer for its dielectric constant and loss.

It should be emphasized that increasing the detector's output by increasing the penetration of its probe inside the waveguide is highly undesirable because of the probe's excessive perturbation of the waveguide fields being measured. Table 5 shows the effect of the depth of penetration on the reflected and transmitted powers. From the data in Table 5 it is clear that a probe penetration of more than 0.01 in. is undesirable. For a small probe penetration, on the other hand, the detector output is too small to drive the A/D converter in our automated system.

TABLE 5. EFFECT OF DEPTH OF PENETRATION ON REFLECTED AND TRANSMITTED POWER WHEN SLOTTED LINE IS TERMINATED BY A MATCHED LOAD

Penetration of probe/height of waveguide	Transmitted power in mW	Reflected power in mW
0.00	1.0	0.0
0.25	0.8	0.1
0.50	0.7	0.15

To further examine these sensitivity problems, we have borrowed a commercial 8-mm wavelength precision slotted waveguide. We plan to examine its sensitivity and the suitability for coupling its output to the reflectometer amplifier and the A/D converter in our automated measurement system. Comparison between our detection system and the one in the precision waveguide will also be made and some modifications (if appropriate) will be made to improve the sensitivity of our system.

It is our present feeling that many of these problems could be alleviated by purchasing a commercial E-band precision slotted waveguide.

In-Vivo Dielectric Measurement Method

For in-vivo measurements, two approaches were analyzed in detail:

1. Discrete mode method. In this approach, admittance of the waveguide radiating into a bigger waveguide containing the biological sample is calculated. Use of waveguide boundaries instead of unbounded space for biological sample greatly simplifies the theory for the admittance calculations. With proper selection of the dimensions of the larger waveguide, one can asymptotically approach the characteristics of the unbounded biological sample. This method is similar to the one described by J. Galejs for a stratified plasma [18].

   In this method, all transverse electric (TE) and transverse magnetic (TM) modes are formulated for smaller and larger waveguides in terms of assumed electric-field distributions at the boundary between two waveguides; then the total z-directed power due to all modes divided by the square of the voltage at the aperture gives the required admittance. Final expression for admittance is similar to equation 1 of reference 18.

2. Continuous mode method. This method is similar to one described by M. C. Decreton and F. E. Gardiol [19]. It calculates the admittance of an open-ended waveguide radiating into the biological sample. Discrete mode expansion is assumed in the waveguide while the continuous mode expansion is assumed for the biological sample. Equation 10 of reference 19 gives admittance by matching boundary conditions at the aperture.

Assuming magnetic current distributions at the aperture corresponding to different modes, the admittance is obtained by applying the Rayleigh-Ritz technique. Numerical calculation of admittance by this method involves $(N - 1)^2$ evaluation of double-surface integrals and inversion of a matrix of dimension $(N - 1) \times (N - 1)$, where N is the number of assumed discrete modes at the aperture. Figure 10 shows the flow chart for finding complex permittivities of biological samples by the methods described above. Admittance calculations will have to be performed differently for these methods, but all other steps are similar. Computer programs were written for implementation of both the methods. One of the two will be chosen eventually by considering the accuracy of predicted complex permittivity and numerical efficiency.

For in-vivo measurements of complex permittivities of biological tissues, we have performed some experiments in the X-band to see the validity of our computer program. We have measured $|\rho|$ and $\angle\phi$ from 9.5 to 11 GHz in steps of 0.1 GHz. Table 6 compares the theoretical and experimental VSWRs and phases for deionized water and 3% saline. Instead of introducing the matching transformer outside the waveguide as described in our last report, a $3\lambda_{g\varepsilon I}/4$ alumina matching transformer is used which is inside the waveguide. This is done because of the convergence problems in the numerical approach for low dielectric constant matching transformers (which are outside the waveguide) that give low VSWRs. It has been found that there is little difference in theoretical and experimental values of VSWRs for deionized water and saline, but the phase differs significantly. Also, there is a small but consistent difference in VSWRs between 3% saline and water in experimental as well as theoretical results.

For the theoretical calculation of the reflection coefficient values given in Table 6, we assumed complex permittivity for deionized water to be as per Debye equation with $\varepsilon_\infty = 4.9$, $\varepsilon_o = 77.0$, and $\tau = 7.5 \times 10^{-12}$ sec, while the assumed complex permittivities for 3% saline are obtained by adding 2.0 to the imaginary part of the complex permittivity values for deionized water. The dielectric constant of the matching transformer, i.e., alumina, is assumed to be 9.3.

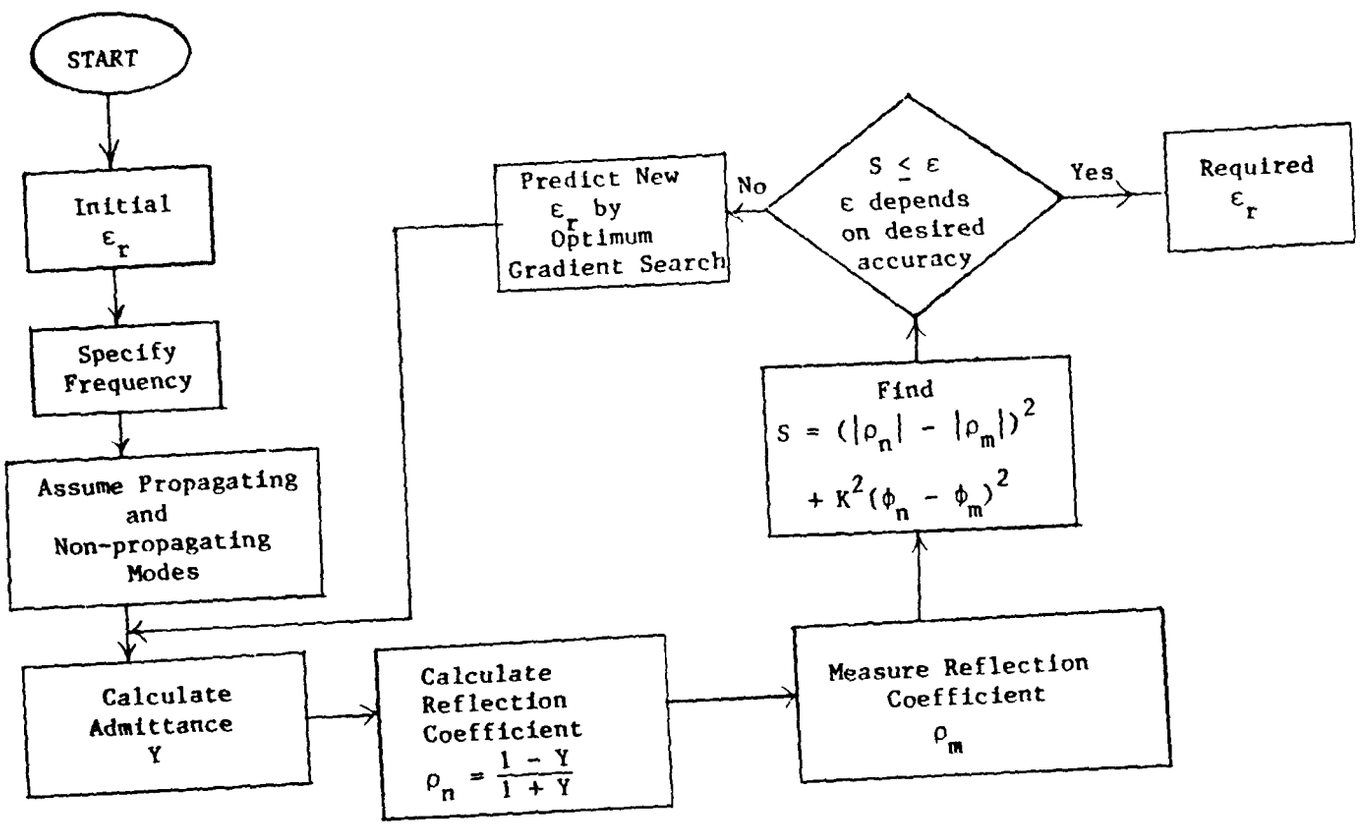

Figure 10. Flow chart of the computer program for in-vivo dielectric measurements.

TABLE 6. THEORETICAL AND EXPERIMENTAL VALUES OF VSWRs AND PHASES FOR DEIONIZED WATER AND 3% SALINE

	Deionized water				3% saline			
	Theoretical		Experimental		Theoretical		Experimental	
Frequency in GHz	VSWR	Phase in degrees	VSWR	Phase in degrees	VSWR	Phase in degrees	VSWR	Phase in degrees
9.5	3.456	145.04	3.311	127.93	3.432	144.60	3.225	126.30
9.7	2.739	141.55	2.729	123.91	2.714	141.03	2.630	123.91
9.9	2.157	140.01	2.125	127.39	2.131	139.46	2.042	129.16
10.1	1.714	144.08	1.688	127.58	1.690	143.75	1.641	133.09
10.3	1.443	163.13	1.419	146.1	1.424	164.07	1.403	153.69
10.5	1.434	198.43	1.401	186.99	1.431	200.67	1.447	194.85
10.7	1.682	218.24	1.620	212.32	1.693	219.56	1.732	212.32
10.9	2.077	222.90	2.037	219.57	2.099	223.61	2.150	219.57

Efforts are underway to analyze the sources of errors in this system that resulted in the discrepancies between the calculated and measured values of the reflection coefficient particularly as regards to the phase.

LASER BRILLOUIN AND RAMAN SPECTROSCOPY OF BIOLOGICAL SYSTEMS

Using the Raman system shown in Figure 11, we have examined some virus suspensions prepared by polyethylene glycol precipitation and rate zonal and density gradient centrifugation. The viruses were vesicular stomatitis virus (VSV), Sindbis virus, and LaCrosse (LaC) viruses. All three viruses were suspended in a tris-NaCl-EDTA buffer whose spectrum was also taken. The spectra were taken in the range 200-3500 cm^{-1} at a scanning speed of 4 cm^{-1}/sec and a time constant of 0.2 sec and recorded on a strip chart recorder.

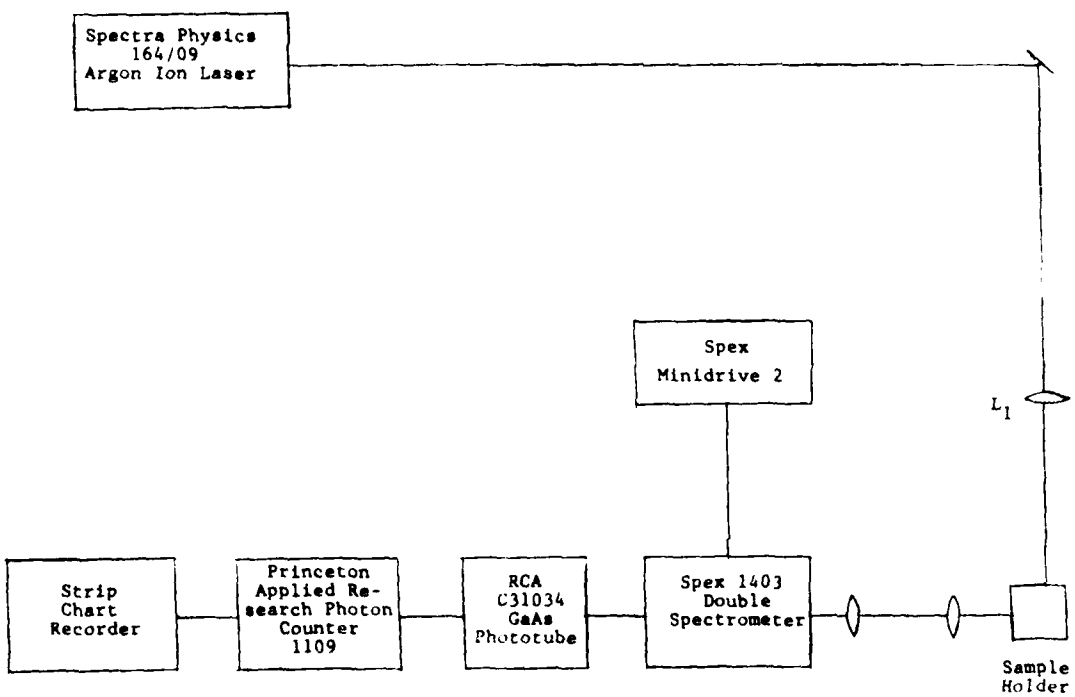

Figure 11. Initial Raman system.

The suspensions were placed in a fused silica cell, at room temperature. Under these conditions, only the VSV suspension gave a Raman spectrum different from the suspending medium. This was because of the much higher concentration of this virus suspension. The Raman peaks were observed at 230, 356, 526, 724, and 1031 cm^{-1}.

A water-jacketed flowing sample holder has been designed and fabricated. This system has been designed to allow simultaneous millimeter-wave irradiation under temperature-controlled conditions.

Interest has been renewed in examining the Raman spectra of Bacillus megaterium. In preliminary experiments following the procedure outlined by Webb [20], we have observed apparent time-dependent Raman lines in the frequency band 800-1800 cm^{-1}. The system used to obtain these spectra is shown in Figure 12, with an integration time of 1 sec and spectral step of 4 cm^{-1}.

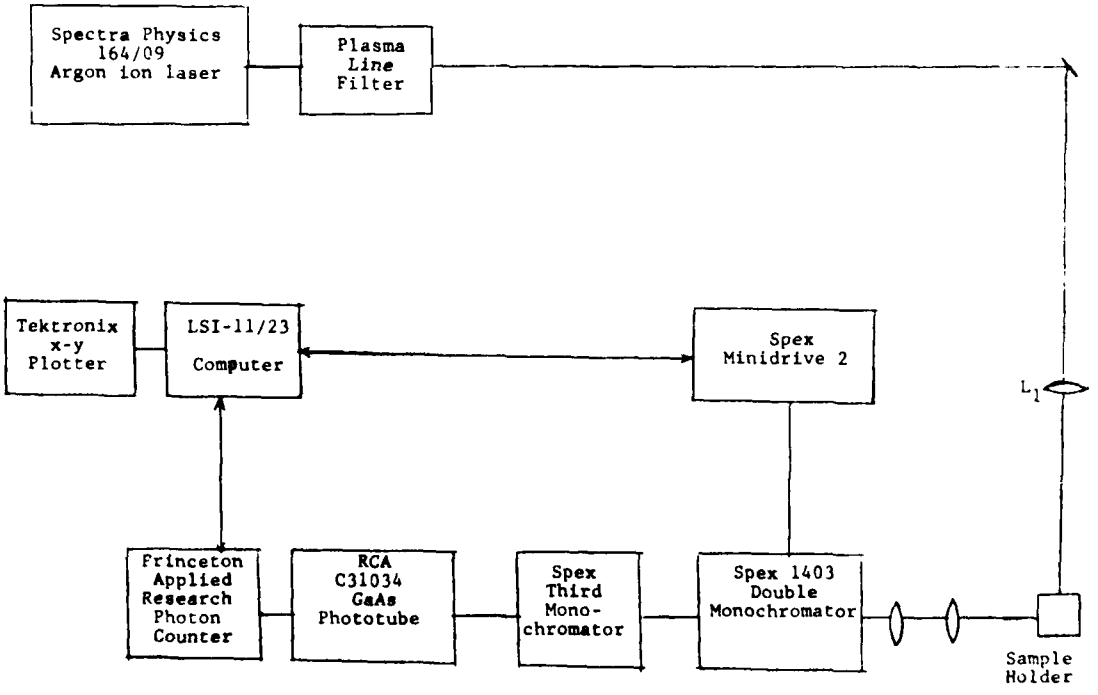

Figure 12. Present Raman system.

A time sequence of the Raman spectra are attached here as Figures 13(a)-(g). At this point, it is not clear whether any artifacts are involved in the appearance of these lines. More work is presently underway to delineate the conditions under which these lines are observed. We also plan to use an optical multichannel system [SPEX Doublemate 0.25-m subtractive dispersion double spectrometer, Princeton Applied Research 1420 intensified diode array detector] to examine whether the Raman shifted emissions are narrow band or broadband and also to examine the dependence of the Raman frequencies.

PROGRESS ON PREPARATION OF THE BIOLOGICAL MEDIA

In the past year, the three viruses prepared to be used for Raman studies, have been investigated extensively. They are vesicular stomatitis virus (VSV), Sindbis virus, and LaCrosse (LaC) virus. They have been propagated in BHK-21 cells to high titer with and without ^{35}S-methionine, ^{32}P, or other appropriate radiolabels. For the proposed Raman light scattering as well as for other studies, it is necessary to use highly homogeneous and monodispersed suspensions. Methods have been adapted to these three viruses which have allowed the preparation of such suspensions using polyethylene glycol precipitation, rate zonal, and density gradient ultra-centrifugation. The suspensions have been found to be highly concentrated and homogeneous by analytical rate zonal centrifugation.

Methods have been developed or adapted for disruption of the viruses and isolation, purification, and analysis of their envelope glycoproteins. These techniques employ nonionic detergent dissociation in high salt, gel exclusion chromatography, and polyacrylamide gel electrophoresis. These methods will be employed to prepare lipid vesicles (liposomes) with specific viral glycoproteins "inserted" in the bilayer.

Extensive studies have been carried out by preparation of a "battery" of monoclonal antibodies to the G1 glycoprotein of the LaC virus. Mice were immunized to both infectious virus and purified G1 glycoprotein. Spleen cells from these mice were fused to myeloma cells and the resulting hybridoma cells selected for and cloned. Over 70 separate, successful clones have been passed and frozen down for future work. Twenty of them have been grown in vitro, injected into mice, and ascitic fluids prepared. Specific immunoglobulins

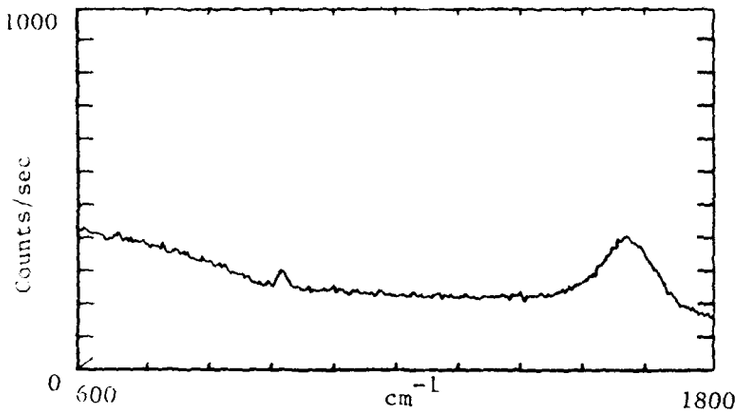

Figure 13a. Raman spectra of Davis Minimal Medium diluted 1:3 in H_2O. This is the medium in which the Bacillus megaterium cultures are resuspended.

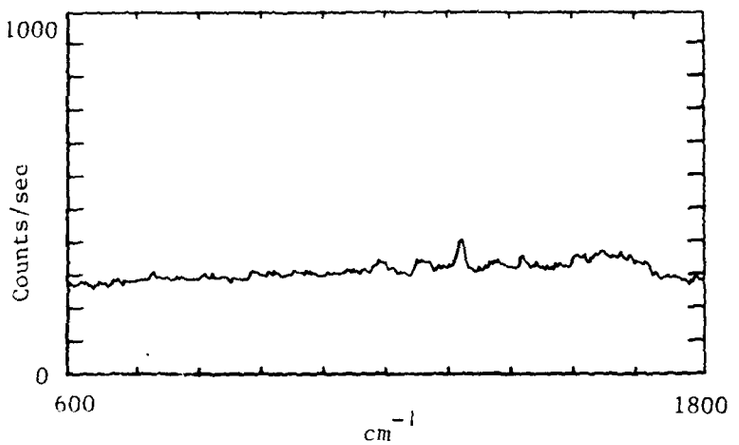

Figure 13b. Raman spectra for cultures of Bacillus megaterium taken 19 min after resuspension.

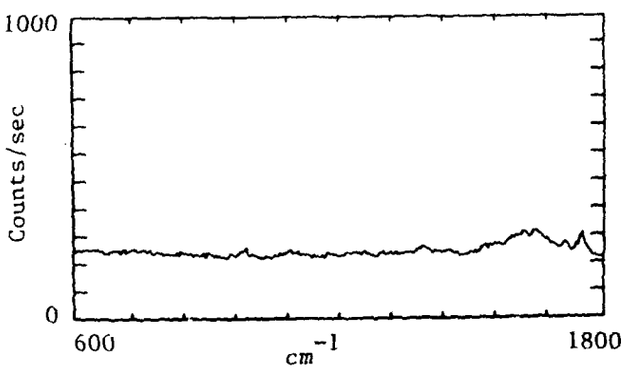

Figure 13c. Raman spectra for cultures of Bacillus megaterium taken 30 min after resuspension.

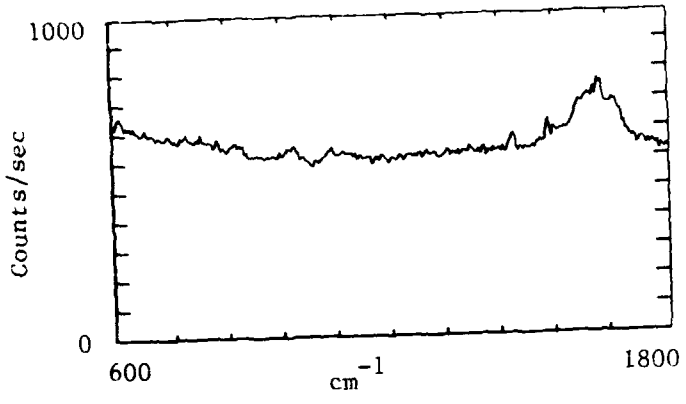

Figure 13d. Raman spectra for cultures of Bacillus megaterium taken 41 min after resuspension.

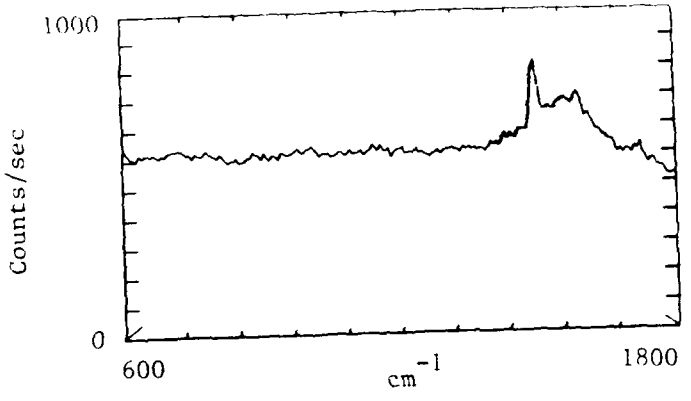

Figure 13e. Raman spectra for cultures of Bacillus megaterium taken 50 min after resuspension.

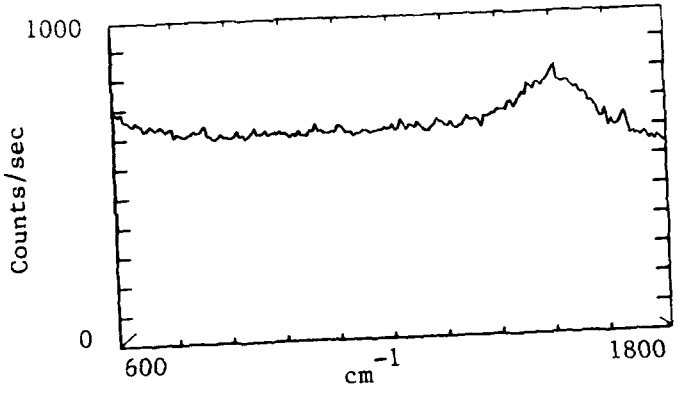

Figure 13f. Raman spectra for cultures of Bacillus megaterium taken 59 min after resuspension.

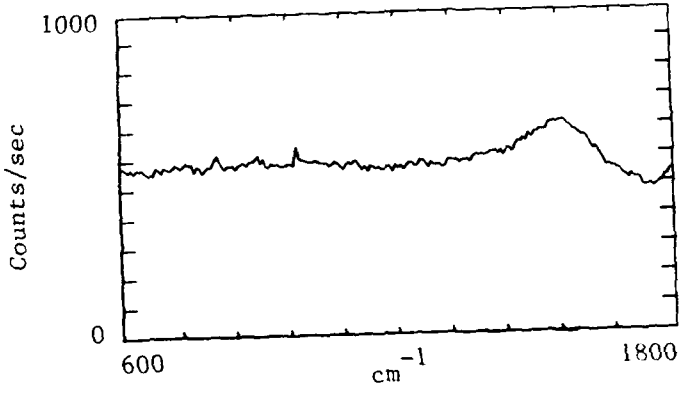

Figure 13g. Raman spectra for cultures of Bacillus megaterium taken 1 hr 50 min after resuspension.

have been isolated, purified, and characterized with respect to isotype, neutralizing and hemagglutination inhibition activities, and ^{125}I-competition binding. These studies have allowed us to map specific antigenic determinants (epitopes) on the G1 glycoprotein of LaC with respect to the trypsin-sensitive cleavage sites. The finding which is of critical importance to new proposed studies on microwave effects on biological structures is that epitope-specific immunoglobulins (antibodies) react with this enveloped viruses' glycoprotein (G1) and cooperatively produce conformational changes in these antibodies and probably the G1 glycoprotein in situ.

REFERENCES

1. Devyatkov, N. D., et al. Highlights of the papers presented on millimeter wave biological effects. Sov Phys--Usp 4:568-579 (1974).

2. Grundler, W., F. Keilmann, and H. Fröhlich. Resonant growth rate response of yeast cells irradiated by weak microwaves. Phys Lett 62A:464-466 (1977).

3. Kremer, F., C. Koschnitzke, L. Santo, P. Quick, and A. Poglitsch. The nonthermal influence of millimeter-wave radiation on the puffing of giant chromosomes. In H. Fröhlich and F. Kremer (eds.). Coherent excitations in biological systems. Berlin-New York: Springer Verlag, 1983.

4. Berteaud, A. J., et al. Action d'un rayonnement electromagnetique a'longuer d'onde millimetrique sur la croissance bacterienne. Comptes Rendus Acad Sci (Paris) 281:843-846 (1975).

5. Partlow, L. M., et al. A novel in vitro method for study of thermal and athermal bioeffects of microwave irradiation on monolayer cultures. Bioelectromagnetics 2:123-140 (1981).

6. Stensaas, L. J., et al. Thermal and athermal bioeffects of microwave irradiation on monolayer cultures of BHK-21/C13 cells assessed by scanning and transmission electron microscopy. Bioelectromagnetics 2:141-150 (1981).

7. Bush, L. G., et al. Lack of frequency-specific athermal microwave bioeffects on protein synthesis by monolayer cultures of BHK-21/C13 cells. Bioelectromagnetics 2:151-160 (1981).

8. Furia, L., et al. Lack of mutagenic effects of millimeter waves on Salmonella typhimurium and on induction of lambda phage. Submitted for publication to Mutation Res.

9. Riazi, A., et al. A broadband temperature-controlled system for the study of cellular bioeffects of microwaves. IEEE Trans Microwave Theory Tech MTT-30:1996-1998 (1982).

10. Szwarnowski, S., and R. J. Sheppard. Precision waveguide cells for the measurement of permittivity of lossy liquids at 70 GHz. J Phys 10E:1163-1167 (1977).

11. Van Loon, R., and R. Finsy. The precise microwave measurements of liquids using a multipoint technique and curve-fitting procedure. J Phys 8D:1232-1243 (1975).

12. Gandhi, O. P., et al. Millimeter-wave absorption spectra of biological samples. Bioelectromagnetics 1:285-298 (1980).

13. Fröhlich, H. Coherent electric vibrations in biological systems and the cancer problem. IEEE Trans Microwave Theory Tech MTT-26:613-617 (1978).

14. Ames, B. N., et al. Methods for detecting carcinogens and mutagens with the Salmonella/mammalian microsome mutogenicity test. Mutation Res 31:347-361 (1975).

15. Ames, B. N. Identifying environmental chemicals causing mutations and cancer. Sci 204:587-593 (1979).

16. Grundler, W. Recent results of experiments on nonthermal effects of millimeter microwaves on yeast growth. Coll Phenom 3:181-186 (1981).

17. Grundler, W., et al. Nonthermal resonant effects of 42-GHz microwave on the growth of yeast culture. In H. Fröhlich and F. Kremer (eds.). Coherent excitations in biological systems. Berlin-New York: Springer Verlag, 1983.

18. Galejs, J. Admittance of a waveguide radiating into stratified plasma. IEEE Trans Anten Prop AP-13:64-70 (1965).

19. Decreton, M. C., and F. E. Gardiol. Simple nondestructive method for the measurement of complex permittivity. IEEE Trans Instrum Meas IM-23:434-438 (1974).

20. Webb, S. J. Laser Raman spectroscopy of living cells. Phys Rev 60(4):201-224 (1980).

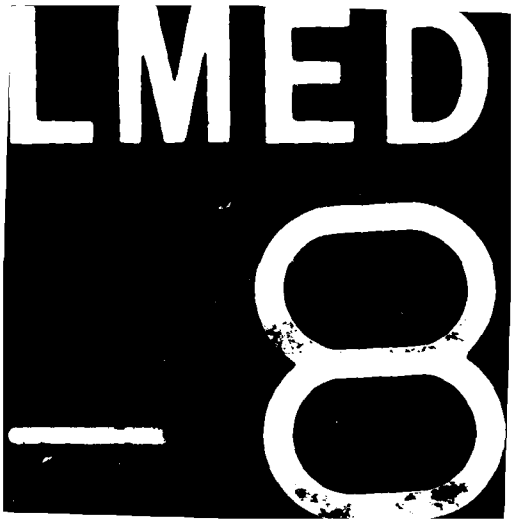
LMED
8